

## Transient Laminar Conjugate Natural Convection in a Cavity with a Finite Thickness and Conductivity Partition

M. Khatamifar<sup>1</sup>, W. Lin<sup>1,2</sup>, D. Holmes<sup>1</sup>, S. W. Armfield<sup>3</sup> and M. P. Kirkpatrick<sup>3</sup>

<sup>1</sup>College of Science and Engineering  
James Cook University, Townsville, QLD 4811, Australia

<sup>2</sup>Solar Energy Research Institute  
Yunnan Normal University, Kunming, Yunnan 650092, China

<sup>3</sup>School of Aerospace Mechanical & Mechatronic Engineering  
The University of Sydney, NSW 2006, Australia

### Abstract

Numerical simulation of transient laminar conjugate natural convection in a differentially heated cavity with a finite thickness and conductivity partition is performed for  $10^5 \leq Ra \leq 10^9$ . The transient flow development in the cavity and the conjugate natural convection boundary layers (CNCBL) on the partition are investigated in detail. Four stages of flow development are identified, namely, an initial rapid start-up stage of the boundary layers on the heated and cooled walls; the filling stage of the left and right enclosures with stratified fluid together with onset of heat transfer through the partition and the development of associated CNCBLs; the transition to stage full development; and the steady state stage.

### Introduction

Transient natural convection flow occurs in many industrial applications and devices. The basic natural convection boundary layer flow, without conjugate heat transfer, has been extensively investigated under a variety of configurations and conditions using theoretical, numerical and experimental approaches (see, e.g., [2, 6]). Many of these applications also include conjugate heat transfer and associated CNCBLs, such as the heat exchanger flows and heat transfer across building windows. A basic model for such flows is the side heated cavity with conducting partition, and a number of studies have also considered this configuration. For example, Williamson and Armfield [7, 8] studied the stability characteristics of conjugate natural convection boundary layers in a differentially heated rectangular cavity, partitioned in the middle by a zero thickness and infinite thermal conductivity wall, and found the critical Rayleigh number for the flow to become oscillatory. Xu *et al.*[10] experimentally investigated the instability properties of CNCBLs and a dependency between the frequency and speed of the travelling waves in the CNCBLs and  $Ra$  number was reported. They also classified unsteady natural convection flows in a partitioned cavity, under the assumption of a thin and infinite thermal conductivity partition, into three distinct stages, that is, the initial, transient and steady state stages. They examined the transient start-up characteristics of unsteady natural convection flows in both sides of the partition and reported that the volumetric flow rate and heat transfer are reduced by 37% and 50%, respectively, due to the presence of the partition [9].

The majority of the past studies have focused on the transient natural convection in a partitioned cavity with the assumption of a thin partition and/or a partition with infinite thermal conductivity and simplified initial thermal conditions. This motivates the present study to examine numerically the transient heat transfer through coupled thermal boundary layers in a partitioned cavity under more realistic assumptions, that is, a parti-

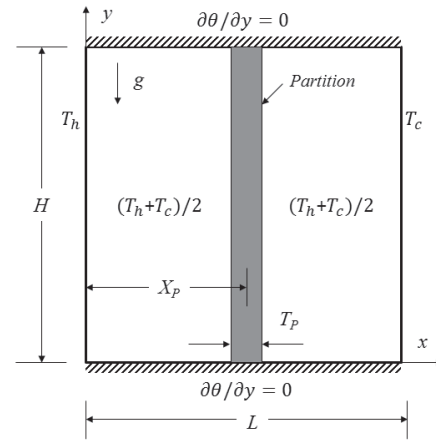


Figure 1: Schematic of the physical model, the computational domain and the boundary conditions.

tion with a finite thickness and conductivity.

### Numerical Method

The physical system under consideration is a two-dimensional differentially heated cavity with height  $H$  and width  $L$ , partitioned by a heat conducting wall of thickness  $T_P$  and thermal conductivity  $k_s$ , as illustrated in figure 1. The top and bottom walls of the cavity are adiabatic and the left and right vertical walls are isothermal at fixed temperatures  $T_h$  and  $T_c$ , respectively ( $T_h > T_c$ ). The partition is placed so that the partition centre is  $X_P$  from the left wall. The working fluid is assumed to be air ( $Pr = 0.71$ ) and initially quiescent and the initial temperature of the fluid and in the partition is  $(T_h + T_c)/2$ . All walls and the partition surfaces are assumed to be rigid and no-slip.

The two-dimensional governing equations for the flow inside the cavity, with the assumption of laminar flow and the Oberbeck-Boussinesq approximation for buoyancy, are written in Cartesian coordinates as follows,

$$\frac{\partial u}{\partial x} + \frac{\partial v}{\partial y} = 0, \quad (1)$$

$$\frac{\partial u}{\partial \tau} + \frac{\partial(uu)}{\partial x} + \frac{\partial(vu)}{\partial y} = -\frac{\partial p}{\partial x} + \sqrt{\frac{Pr}{Ra}} \left( \frac{\partial^2 u}{\partial x^2} + \frac{\partial^2 u}{\partial y^2} \right), \quad (2)$$

$$\frac{\partial v}{\partial \tau} + \frac{\partial(uv)}{\partial x} + \frac{\partial(vv)}{\partial y} = -\frac{\partial p}{\partial y} + \sqrt{\frac{Pr}{Ra}} \left( \frac{\partial^2 v}{\partial x^2} + \frac{\partial^2 v}{\partial y^2} \right) + \theta, \quad (3)$$

$$\frac{\partial \theta}{\partial \tau} + \frac{\partial(u\theta)}{\partial x} + \frac{\partial(v\theta)}{\partial y} = \sqrt{\frac{1}{RaPr}} \left( \frac{\partial^2 \theta}{\partial x^2} + \frac{\partial^2 \theta}{\partial y^2} \right), \quad (4)$$

where  $x$  and  $y$  are the dimensionless coordinates,  $u$  and  $v$  are the dimensionless velocity components in the  $x$  and  $y$  directions,  $\tau$ ,  $p$  and  $\theta$  are the dimensionless time, pressure and temperature, respectively, all made dimensionless by their respective scales as follows,

$$\begin{aligned} x = \frac{X}{H}, y = \frac{Y}{H}, u = \frac{U}{U_{ref}}, v = \frac{V}{U_{ref}}, \tau = \frac{U_{ref}}{H} t, \\ p = \frac{P}{\rho_f U_{ref}^2}, \theta = \frac{T - T_c}{T_h - T_c}, \end{aligned} \quad (5)$$

in which  $X, Y, U, V, t, P$ , and  $T$  are the dimensional counterparts of  $x, y, u, v, \tau, p$  and  $\theta$ , respectively, and  $\rho_f$  is the density of the fluid. The velocity scale is  $U_{ref} = \frac{\alpha_f}{H} \sqrt{PrRa}$ , with the Prandtl number ( $Pr$ ) and the Rayleigh number ( $Ra$ ) defined as follows,

$$Pr = \frac{\nu_f}{\alpha_f}, \quad Ra = \frac{g\beta_f(T_h - T_c)H^3}{\nu_f\alpha_f}, \quad (6)$$

in which  $g$  is the acceleration due to gravity, and  $\nu_f, \alpha_f$  and  $\beta_f$  are the kinematic viscosity, thermal diffusivity and the coefficient of volumetric expansion of the fluid, respectively.

The heat transfer within the heat-conducting partition is governed by the following dimensionless equation,

$$\frac{\partial\theta}{\partial\tau} = \frac{k_r}{\sqrt{RaPr}} \left( \frac{\partial^2\theta}{\partial x^2} + \frac{\partial^2\theta}{\partial y^2} \right), \quad (7)$$

where  $k_r$  is the thermal conductivity ratio between the solid partition and the fluid in the cavity, defined as follows,

$$k_r = \frac{k_s}{k_f} \quad (8)$$

in which  $k_f$  and  $k_s$  are the thermal conductivities of the fluid and the partition, respectively.

The initial conditions at  $\tau = 0$  are  $u = v = 0$  and  $\theta = 0.5$  everywhere within the cavity (except sidewalls) and also in the partition, and for  $\tau > 0$  the boundary conditions for the fluid are  $u = v = 0$  on all solid surfaces,  $\partial\theta/\partial y = 0$  on the top and bottom walls, and  $\theta = 1$  and  $\theta = 0$  on the left and right vertical walls, respectively, and the boundary conditions for the partition wall are,

$$u = v = 0, \quad k_r \left( \frac{\partial\theta}{\partial x} \right)_{x_1^-} = \left( \frac{\partial\theta}{\partial x} \right)_{x_1^+}, \quad \text{at } x = x_1, \quad (9)$$

$$u = v = 0, \quad k_r \left( \frac{\partial\theta}{\partial x} \right)_{x_2^-} = \left( \frac{\partial\theta}{\partial x} \right)_{x_2^+}, \quad \text{at } x = x_2, \quad (10)$$

where  $x_1$  and  $x_2$  are the locations of the left and right sides of the partition wall and the associated superscripts '-' and '+' denote their nearest left and right cells, respectively.

The above governing equations (1) to (4) and (7) were discretized using the finite volume method with the SIMPLE algorithm used to obtain the pressure and enforce continuity. The QUICK scheme was used for the advection terms and second-order central differences for all other spatial terms. The momentum and temperature equations are integrated in time used the second-order Adams-Bashforth scheme. An in-house direct numerical simulation (DNS) code written in Visual C# was developed and used to solve the discretized governing equations. Non-uniform Cartesian grids in both the  $x$  and  $y$  directions were constructed using a sine function, with coarser grids in the core regions and finer grids concentrated in the proximity of the partition and cavity boundary walls. Grid dependence tests have

been conducted on two grid systems of  $200 \times 200$  and  $300 \times 250$  cells, at time-step sizes  $\Delta\tau = 0.0001$  and  $0.0005$ , with only small variation observed in the temperature time-series. Hence, to capture the transient features of flow development and boundary layers, the  $300 \times 250$  grid system and  $\Delta\tau = 0.0001$  time-step are used in this study.

## Results

The transient features of the natural convection flow in a partitioned cavity, including the development of the conjugate natural convection boundary layers, general flow structure and behaviour, are characterised in this section for the dimensionless partition thickness of  $T_p = 0.05$ , dimensionless partition position of  $X_p = 0.5$ ,  $k_r = 622$ ,  $H/L = 1$ ,  $10^5 \leq Ra \leq 10^9$  and  $Pr = 0.71$ .

Figure 2 presents the temperature contours at five different times for the left half of the cavity (due to symmetry, the results for the right enclosure have not been presented with different  $Ra$  values). At the initial stage a rising natural convection boundary layer forms on the left-hand side wall of the half-cavity, discharging heated fluid as an intrusion below the ceiling. This can be seen for all  $Ra$  at  $\tau = 5$ . For the higher Rayleigh numbers,  $Ra = 1 \times 10^8$  and  $Ra = 1 \times 10^9$  hot intrusion has not reached the partition on the right hand side of the half-cavity, and the fluid in the remainder of the domain is still at the initial temperature  $\theta = 0.5$ . At  $\tau = 10$ , the heated intrusions discharged by the rising natural convection boundary layers have impinged on the partition, for all  $Ra$  values, and are in the process of filling the half-cavity with hotter fluid. This process is more rapid for the lower  $Ra$ , which have thicker boundary layers and associated higher discharge rates. For the highest  $Ra$  value  $Ra = 1 \times 10^9$ , only a small proportion of the half cavity is filled with discharged hotter fluid. This filling processes continues as shown at  $\tau = 50$ . The heated fluid in the left half-cavity is in contact with the partition, producing temperature difference across the partition, and producing, in the left half-cavity, a falling conjugate natural convection boundary layer discharging into a cool intrusion at the bottom of the half-cavity, enhancing the process of stratification. The process of stratification is largely complete for all  $Ra$  at  $\tau = 100$ , with a stable stratification spanning the full height of the half-cavities, and the falling conjugate natural convection boundary layers well established on the partition. Some further development is seen in the two high  $Ra$  cases, up to  $\tau = 300$ , when the flow has reached a fully developed steady-state for all  $Ra$  cases.

For  $Ra = 1 \times 10^5$ , the lowest  $Ra$  value considered, at full development the temperature on the vertical centre line of the half-cavity ( $x = 0.25$ ) ranges from  $\theta \cong 1.0$  at the top to  $\theta \cong 0.5$  at the bottom. At the highest Rayleigh number  $Ra = 1 \times 10^9$  the variation is reduced, with  $\theta = 1.0$  at the top at  $\theta \cong 0.7$  at the bottom. This variation is significantly smaller than corresponding non-partitioned cavity, where the variation is approximately 1.0 [4], and is a result of the partition blocking the flow of fluid across the cavity and thereby limiting the advective heat transfer.

The high  $Ra$  flows are observed to be considerably more active with more complex spatial structure during development, as compared to the low  $Ra$  flows. As well as the reduced natural convection boundary layer thickness noted above, the high  $Ra$  cases display wave-breaking structures when the hot intrusion initially strikes and interacts with the partition, seen in the temperature contours at  $\tau = 10$ . This behaviour is similar to that observed in the equivalent non-partitioned cavity, and reduces with time as the cavity becomes filled and stratified. The equivalent non-partitioned cavity at  $Pr = 0.71$  undergoes a bifurcation to an unsteady flow at full development at

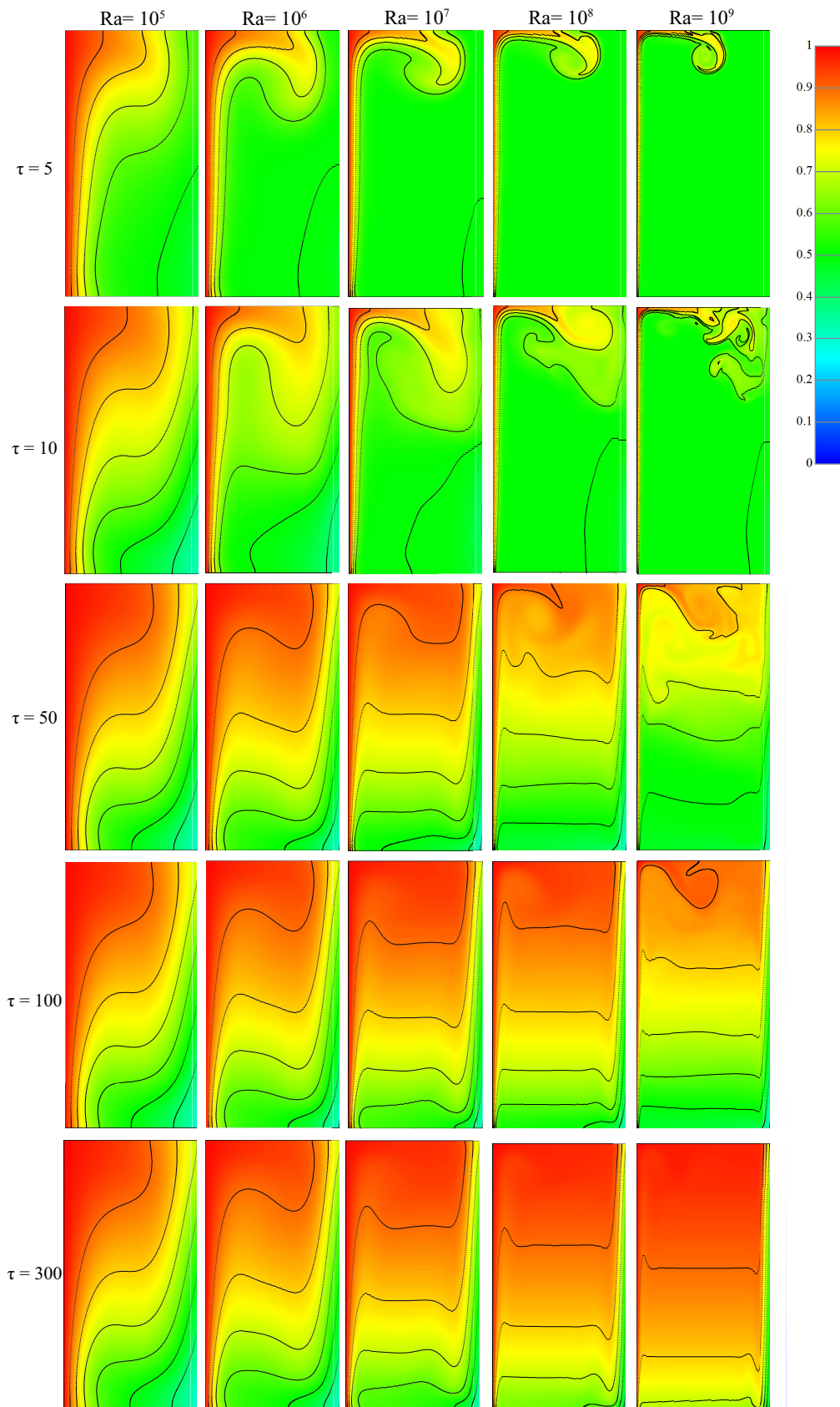


Figure 2: Temperature contours on the left enclosure at different times.

$Ra \sim 1.83 \times 10^8$  [5] whereas the partitioned cavity flow considered here is steady at full development at the higher value of  $Ra = 1 \times 10^9$ . It is hypothesised that the partition, in acting to reduce the heat transfer, reduces the effective Rayleigh number of the flow, and so increasing the critical Rayleigh number for bifurcation to unsteady flow. This observation has also been reported by Ghosh *et al.* [1] who noted that the partition delays the transition to turbulence.

The presence of the upper boundary of the cavity forces both thermal and viscous vertical boundary layers adjacent to isothermal walls to discharge into the core region of the cavity which is similar to the heating-up or cooling-down process. It is appropriate to assume the heating-up process in the left enclosure or the cooling-down process in the right enclosure separately. Lin *et al.* [3] have presented a scaling relation of  $\tau_s \propto Ra^{1/4}$  (where  $\tau_s$  represents the time for the flow in the cavity to attain steady-state. It is determined at the time when the average Nusselt number of the sidewalls and the partition reach to the same value.) for the cooling-down stage in a rectangular cavity without partition. Although this scaling was originally developed for a non-partitioned cavity, it is also examined here for the partitioned cavity to study to what extent the effect of the conducting partition can be neglected. The scaling is seen to perform well for partitioned cavity as  $\tau_s \propto Ra^{1/4}$  shows almost linear relation in figure 3(c). To investigate more,  $\tau_{o,y}$  is defined as onset time for stratification at height  $y$ . To evaluate this parameter, 19 equally-spaced points were selected for each  $Ra$  number at the middle of the left enclosure and the reported time is when the absolute difference value of the temperature between the point and the initial temperature was bigger than 0.01. Figure 3 (a) shows  $\tau_{o,y} \propto y$  and it can be seen that as  $Ra$  value increases delay for the onset of stratification increases. The early temperature difference at some points (e.g. (0.25, 0.05) for  $Ra = 10^9$ ) is because of earlier heat transferring through the partition and earlier reaching lower temperature of cold wall to the left enclosure. The scaling  $\tau_{o,y}/Ra^{1/4} \propto y$  is presented in figure 3 (b). This scaling almost brings all the stratification onset graphs onto a single graph indicating that the results of local stratification onset obtained for the partitioned cavity obey the stratification scaling relation of the cooling-down process. For the case of  $Ra = 10^5$  the results are affected by the thick thermal boundary layer and subsequently the obtained stratification onset data may not have enough accuracy.

## Conclusions

In this paper, the CNCBLs induced in a differentially heated partitioned cavity are investigated numerically. The transient features of natural convection flows in the centrally partitioned cavity as well as the subsequent CNCBLs are identified. Four distinct stages have been identified to characterise the development of natural convection flows in the partitioned cavity.

## Acknowledgements

The support from the Australian Research Council, the National Natural Science Foundation of China (51469035, 51266016) and James Cook University is gratefully acknowledged.

## References

- [1] Ghosh, P.K., Sarkar, A. and Sastri, V.M.K., Natural convection heat transfer in an enclosure with a partition a finite-element analysis, *Numerical Heat Transfer Applications*, **21**, 1992, 231–248.
- [2] Khalilollahi, A. and Sammakia, B., Unsteady natural convection generated by a heated surface within an enclosure,

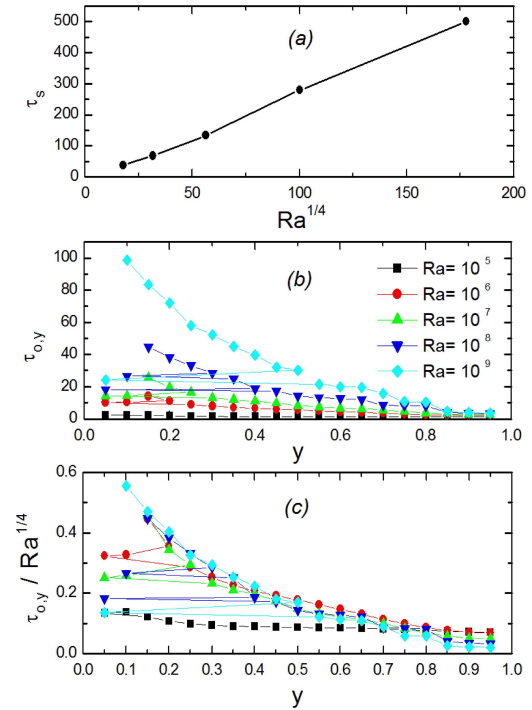


Figure 3: (a)  $\tau_{o,y} \sim y$  and (b)  $\tau_{o,y}/Ra^{1/4} \sim y$  at 19 equally-spaced points at the middle of the left enclosure and (c)  $\tau_s \sim Ra^{1/4}$  for the whole left enclosure.

*Numerical Heat Transfer*, **9**, 1986, 715–730.

- [3] Lin, W., Armfield, S.W. and Patterson, J.C., Cooling of a  $Pr < 1$  fluid in a rectangular container, *Journal of Fluid Mechanics*, **574**, 2007, 85–108.
- [4] Patterson, J.C. and Imberger, J., Unsteady natural convection in a rectangular cavity. *Journal of Fluid Mechanics*, **100**, 1980, 65–86.
- [5] Quere, P.L. and Behnia, M., From onset of unsteadiness to chaos in a differentially heated square cavity, *Journal of Fluid Mechanics*, **359**, 1998, 81–107.
- [6] Szekely, J. and Todd, M., Natural convection in a rectangular cavity transient behaviour and two phase systems in laminar flow, *International Journal of Heat and Mass Transfer*, **14**, 1971, 467–482.
- [7] Williamson, N. and Armfield, S.W., Stability characteristics of conjugate natural convection boundary layers, *ANZIAM Journal*, **52**, 2011, 696–709.
- [8] Williamson, N., Armfield, S.W. and Kirkpatrick, M.P., Transition to oscillatory flow in a differentially heated cavity with a conducting partition, *Journal of Fluid Mechanics*, **693**, 2012, 93–114.
- [9] Xu, F., Patterson, J.C. and Lei, C., Heat transfer through coupled thermal boundary layers induced by a suddenly generated temperature difference, *International Journal of Heat and Mass Transfer* **52**, 2009, 4966–4975.
- [10] Xu, F., Patterson, J.C. and Lei, C., An experimental study of the coupled thermal boundary layers adjacent to a partition in a differentially heated cavity, *Experimental Thermal and Fluid Science*, **54**, 2014, 12–21.